行政院國家科學委員會專題研究計畫　成果報告

新的微波濾波器耦合參數萃取與診斷方法之開發與驗證

計畫類別： 個別型計畫
計畫編號： NSC94-2213-E-009-072-
執行期間： 94 年 08 月 01 日至 95 年 07 月 31 日
執行單位： 國立交通大學電信工程學系(所)

計畫主持人： 張志揚

計畫參與人員： 廖竟谷，紀鈞翔，紀佩&#32491；，陳永順

報告類型： 精簡報告
報告附件： 出席國際會議研究心得報告及發表論文
處理方式： 本計畫可公開查詢

中　華　民　國 95 年 9 月 18 日

新的微波濾波器耦合參數萃取與診斷方法之開發與驗證

計畫編號: 94-2213-E-009-072

執行期限:94 年 8 月 1 日至 95 年 7 月 31 日

張志揚

國立交通大學電信工程系

新竹市大學路 1001 號

中文摘要:本計畫擬研究一個濾波器參數萃取與濾波器診斷的新方法。此方法擬由電磁模擬所得之任意濾波器散射參數來萃取此濾波器之網路參數(耦合矩陣)。我們擬先由哥西法求出S_{11} 與 S_{21}的分式函數之多項式係數然後利用解析方式求出橫向耦合矩陣之各矩陣元素。經由多重相似轉換可將橫向耦合矩陣轉換成與實際濾波器耦合型式相對應的耦合矩陣。此組多重相似轉換之旋轉角可以經由快速且有效的數值最佳化過程來決定。此種新方法之有效性將由實作微帶線四角互耦濾波器加以驗證。。

英文摘要: In this program, a novel technique for extraction of general filter network model parameters (coupling matrix) from scattering parameters obtained via EM simulation is proposed. The coefficients of the polynomials of the rational functions S_{11} and S_{21} are found by applying the Cauchy method. Then, the corresponding transversal coupling matrix is obtained analytically. To obtain coupling matrix with topology corresponding to the physical structure, a multiple similarity transform is proposed to apply to the starting transversal coupling matrix. A set of rotation angles in the multiple similarity transform is determined by means of an efficient and fast optimization procedure. The validity of the proposed scheme will be tested by a microstrip quadruplet filter.

關鍵詞:診斷，交錯耦合，微帶濾波器，傳輸零點。

Key words: Diagnosis, Cross-coupled, microstrip filters, transmission zeros

Ⅰ. Introduction

Microwave filters incorporating the generalized Chebyshev class of filtering functions have found wide applications in both satellite and terrestrial communication systems. A great deal of effort has been made, over past three decades, in analytically synthesizing filter coupling matrix according to an adequate topology with an optimal cost model. The most recent contribution to this subject would be R.J. Cameron's work [1].

Once the required coupling matrix and filter topology are synthesized, physical realization of the filter would largely rely on a costly, experience-based and intricate tuning. It is well known that the core task in filter tuning is a diagnosis of the filter coupling status that corresponds to the current filter response, which could be in various shapes. By comparing the designed circuit model and parameters (i.e. coupling matrix) against the diagnosed ones, the tuning direction and magnitude can be easily decided. Note that the diagnosed parameters must have relevance with those of the designed.

To identify all parameters corresponding to cross couplings, frequency alignment, and source-load coupling, powerful CAD tools are needed. Recently, an elegant diagnosis method is proposed to help designing of symmetric coupled-resonator filters [2]. However, the method in [2] has not taken the source-load coupling into account. In this program, we propose a diagnosis scheme, which is applicable to arbitrary topologies with or without source-load coupling.

Ⅱ. The CAD method for filter diagnosis

The extraction method proposed here has two major steps. In the first step, we extract the (N+2)×(N+2) transversal coupling matrix, for the filter of order N, from the EM simulated response as Alejandro et al. have done in [3]. In [3], the authors apply the Cauchy method to get the rational polynomial approximation of $S_{11}(\Omega)$ and $S_{21}(\Omega)$ from the EM simulated results, and then generate the corresponding transversal coupling matrix by the method proposed by Cameron [1]. Extracting the coefficients of the rational function by Cauchy method is attractive since there is no need of calibrating the reference plane as that in [2, 4]. In this step, we would get the transversal coupling matrix like the follows (take the quadruplet filter for instance).

$$M=\begin{bmatrix} 0 & M_{S1} & M_{S2} & M_{S3} & M_{S4} & M_{SL} \\ M_{S1} & M_{11} & 0 & 0 & 0 & M_{1L} \\ M_{S2} & 0 & M_{22} & 0 & 0 & M_{2L} \\ M_{S3} & 0 & 0 & M_{33} & 0 & M_{3L} \\ M_{S4} & 0 & 0 & 0 & M_{44} & M_{4L} \\ M_{SL} & M_{1L} & M_{2L} & M_{3L} & M_{4L} & 0 \end{bmatrix} \quad (1)$$

The equivalent circuit of the transversal network with M-matrix in Eqn.(1) is shown in Fig.1 (a). The coupling matrix is related to the responses of $S_{11}(\Omega)$ and $S_{21}(\Omega)$ via the following equation [5]

$$S_{11}=1+2j[A^{-1}]_{11} \quad (2)$$

$$S_{21}=-2j[A^{-1}]_{N+2,1} \quad (3)$$

Here, $A=\Omega[U_0]+[M]-j[R]$, $\Omega=(f_0/\Delta f)(f/f_0-f_0/f)$, $[U_0]$ is similar to the (N+2)×(N+2) identity matrix except that $[U_0]_{11}=[U_0]_{N+2,N+2}=0$, $[M]$ is the (N+2) × (N+2) symmetric coupling matrix, f_0 is the center frequency of the filter and Δf is its bandwidth, and $[R]$ is the diagonal matrix $[R]=diag\{1,R_{loss},...,R_{loss},1\}$. R_{loss}, which value is $\frac{f_0}{\Delta f}\frac{1}{Q_u}$, accounts for the resonator loss. Q_u is the unloaded quality factor of the resonator. Note that R_{loss} is set to be zero in the filter parameter extraction process since the assumption of lossless network must be satisfied in the extraction of $S_{11}(\Omega)$ and $S_{21}(\Omega)$ [3]. After getting the coupling matrix of prescribed topology, one can put the R_{loss} back to calculate the practical filter response.

In the second step, the transversal coupling matrix is transformed into the prescribed topology. It is known that by applying the multiple similar transformations to the coupling matrix, one can get the equivalent coupling matrix with the same electrical performance as the original coupling

matrix. Some methods may be found in the literature, which describe how to find the sequence of rotations (and the corresponding angles) required for obtaining a few specific topologies [1, 6, 7]. However, to the best of authors' knowledge, how to transfer the transversal coupling matrix into the topology shown in Fig.2 is still not known. Fortunately, one can apply the numerical optimization technique to determine the sequence and rotation angles of the multiple similarity transformations as Macchiarella has done in [8]. The method, reported in [8], works well for the synthesis of a filter with order up to 12. The initial coupling matrix being used in [8] is the canonical folded form or generic form, which corresponds to the filter of order N with maximum of N-2 finite transmission zeros.

In this paper, we apply the optimization method as proposed by Macchiarella to transform the transversal coupling matrix to the prescribed topology. Note that using the transversal coupling matrix as initial coupling matrix extends the method of [8] applicable to a filter of order N with maximum of N finite transmission zeros. In the follows, we take the quadruplet filters with coupling route shown in Fig. 1(b) as an example since it will be used in the next section. Applying the multiple similar transformations to the transversal coupling matrix M in Eq. (1), we would get the new coupling matrix $\overline{M}$ and $\overline{M}$ can be expressed as

$$\begin{aligned}\overline{M} &= (R_{23}\cdot R_{24}\cdot R_{25}\cdot R_{34}\cdot R_{35}\cdot R_{45}) \\ &\quad\cdot M\cdot ({R_{45}}^{t}\cdot {R_{35}}^{t}\cdot {R_{34}}^{t}\cdot {R_{25}}^{t}\cdot {R_{24}}^{t}\cdot {R_{23}}^{t}) \\ &= S(\vartheta_{23},\vartheta_{24},..,\vartheta_{45})\cdot M\cdot S^{t}(\vartheta_{23},\vartheta_{24},..,\vartheta_{45})\end{aligned} \tag{4}$$

where $R_{ij}(\vartheta_{ij})$ is the rotation matrix of order N+2 corresponding to pivot (i, j), and angle ϑ_{ij}. $R_{ij}(\vartheta_{ij})$ is defined as follows:

$$\begin{aligned}&R_{ij}(i,i) = R_{ij}(j,j) = \cos(\vartheta_{ij}) \\ &R_{ij}(i,j) = -R_{ij}(j,i) = \sin(\vartheta_{ij}) \\ &R_{ij}(k,k)\big|_{k\neq i,j} = 1 \qquad ,(i<j)\neq 1,N+2 \\ &R_{ij}(k,i)\big|_{k\neq i,j} = 0 \qquad ,R_{ij}(j,k)\big|_{k\neq i,j} = 0\end{aligned} \tag{5}$$

The cost function U for the topology shown is Fig. 1(b) is defined as

$$\begin{aligned}&U(\vartheta_{23},\vartheta_{24},..,\vartheta_{45}) \\ &=|\overline{M}_{S2}|^2+|\overline{M}_{S3}|^2+|\overline{M}_{2L}|^2+|\overline{M}_{3L}|^2 \\ &+|\overline{M}_{11}-\overline{M}_{44}|^2+|\overline{M}_{22}-\overline{M}_{33}|^2 \\ &+|\overline{M}_{13}-\overline{M}_{24}|^2+|\overline{M}_{S4}-\overline{M}_{1L}|^2\end{aligned} \tag{6}$$

The first four terms in the cost function indicate which cross coupling elements must vanish while the last four terms indicate the symmetry of the coupling route. If the symmetric condition was not included in the cost function, we might get the non-physical solutions. In the practical implementation of the minimization procedure, the Gauss-Newton method is used to determine the rotation angles $(\vartheta_{23},\vartheta_{24},..,\vartheta_{45})$, which minimize the cost function U. Once the rotation angles are determined, we can get the corresponding coupling matrix $\overline{M}_{\mathrm{model}}$.

It should be mentioned that the proposed extraction scheme could be applied to arbitrary topologies once their feasibility has been assessed. Depending on the setting of different cost functions, different topologies can be obtained after multiple similar transformations. For the filter of order N, one can choose the N × N coupling matrix or (N+2) × (N+2) coupling matrix as the initial coupling matrix, depending on the maximum number of finite transmission zeros. If the maximum number of

finite transmission zeros is less than N-2, either N×N [8] or (N+2)×(N+2) coupling matrix [9] can be chosen. Otherwise, the (N+2) × (N+2) transversal coupling matrix should be applied.

Ⅲ. FILTER DESIGN EXAMPLES

In this section, we will focus on development two novel quadruplet filters with source-load coupling and utilize the CAD tool introduced in previous section to do diagnosis of proposed filters. The design procedures are summarized as following. Follows the synthesis method described in [1], one would get the ideal coupling matrix with the topology shown in Fig 2. The corresponding spacing between every resonator is determined through the characterization of the couplings as described in chapter 8 of [10]. After EM simulation, the values of unwanted cross couplings are extracted. Fixing the values of unwanted couplings, the optimization technique is then applied to determining the required frequency shifts of resonators and the change of other coupling elements to compensate the distortion of $|S_{11}|$. Two examples are given to show the design procedures. The first filter, shown in Fig. 3, is designed to have two pairs of real frequency transmission zeros at normalized frequency $\Omega = \pm 2, \pm 6$ for skirt selectivity. The second filter, shown in Fig. 6, is intended to have one pair of real frequency transmission zero at normalized frequency $\Omega = \pm 4.5$ for selectivity and another pair at $\Omega = \pm j1.55$ for in-band flap group delay. The center frequency, the fractional bandwidth, and the maximum in-band return loss of both filters are 2.4GHz, 3.75% and 20dB respectively. The filters are built on a 20-mil-thick Rogers RO4003 substrate with $\varepsilon_r = 3.38$, $\tan\delta = 0.0021$. The commercial EM simulation software Sonnet 9.0 [11] is used to perform the simulation.

A. QUADRUPLET FILTER WITH TWO PAIR OF REAL FREQUENCY TRANSMISSION ZEROS

In order to see the effect of the controlling line, we exclude the controlling line at first and adjust the quadruplet filter following the previously mentioned procedures. After extracting the unwanted diagonal cross couplings of the quadruplet filter and compensate them, we would get the EM simulated response shown as circles in Fig. 5(a). Using the CAD tool developed in section Ⅲ together with the cost function defined in Eq. (6), the extracted coupling matrix M_1 (with the value of cost function $U = 10^{-7}$) is obtained as following.

$$M_1 = \begin{bmatrix} 0 & 1.0089 & 0 & 0 & 0 & 0 \\ 1.0089 & -0.0021 & 0.8514 & -0.0090 & -0.1436 & 0 \\ 0 & 0.8514 & 0.0317 & 0.7380 & -0.0090 & 0 \\ 0 & -0.0090 & 0.7380 & 0.0317 & 0.8514 & 0 \\ 0 & -0.1436 & -0.0090 & 0.8514 & -0.0021 & 1.0089 \\ 0 & 0 & 0 & 0 & 1.0089 & 0 \end{bmatrix}$$

The corresponding response of M_1 is also shown in Fig. 4(a) as solid line for comparison.

After adding the controlling line of source-load coupling, the EM simulated response is shown in Fig. 4(b) as circles. The corresponding extracted coupling matrix M_2 (with the value of cost function $U = 10^{-7}$) is

$$M_2 = \begin{bmatrix} 0 & 1.0189 & 0 & 0 & 0.0032 & 0.0035 \\ 1.0189 & -0.0120 & 0.8572 & -0.0057 & -0.1420 & 0.0033 \\ 0 & 0.8572 & 0.0204 & 0.7390 & -0.0058 & 0 \\ 0 & -0.0057 & 0.7390 & 0.0204 & 0.8571 & 0 \\ 0.0032 & -0.1420 & -0.0058 & 0.8571 & -0.0120 & 1.0189 \\ 0.0035 & 0.0033 & 0 & 0 & 1.0189 & 0 \end{bmatrix}$$

The corresponding response of coupling matrix M_2 is also shown in Fig. 4(b) as solid line.

Comparing M_1 and M_2, it can be easily observed that the introduction of controlling line is only a small perturbation to the original quadruplet. In other words, the controlling line has negligible contribution to the passband response. Besides, the existence of the tiny unwanted diagonal cross couplings M_{S4} and M_{L1} in matrix M_2 explain why the response is asymmetric because the response becomes symmetric as the M_{S4} and M_{L1} are excluded from M_2. Taking matrix M_2 into equation (2) and (3), and setting unloaded quality factor $Q_u = 150$, the results are shown in Fig. 5 as dashed lines. The measured responses are also shown in Fig. 5 as solid lines. Comparing the circuit model responses with measured responses an excellent fit can be observed except some frequency drift toward lower frequency.

B. QUADRUPLET FILTER FOR FLAP GROUP DELAY AND SKIRT SELECTIVITY

As mentioned in section Ⅱ, the unwanted cross couplings M_{13} and M_{24} would destroy the in-band group delay flatness. To reduce the strength of unwanted couplings, we use the L-shaped resonator and arrange the resonators in square to maximize the distance between diagonal resonators as shown in Fig. 7. The coupled lines with length L_1, L_2, and L_3 control the strength of coupling between L-shape resonators respectively. The inductive source-load coupling is effectively controlled by changing the length of controlling line with both ends connected to ground. Resonant frequencies of resonators can be tuned by adjusting the length h1 and h2. Following similar procedures in the previous design, we can get the extracted coupling matrix M_3 as

$$M_3 = \begin{bmatrix} 0 & -1.0945 & 0 & 0 & 0.0052 & 0.0099 \\ -1.0945 & 0.3663 & -1.0093 & -0.0274 & -0.1681 & 0.0054 \\ 0 & -1.0093 & 0.3402 & -0.6241 & -0.0272 & 0 \\ 0 & -0.0274 & -0.6241 & 0.3404 & -1.0089 & 0 \\ 0.0052 & -0.1681 & -0.0272 & -1.0089 & 0.3664 & -1.0936 \\ 0.0099 & 0.0054 & 0 & 0 & -1.0936 & 0 \end{bmatrix}$$

The corresponding response of M_3 fit well with the EM simulated results as shown in Fig.8. Taking M_3 into equation (2) and (3) and setting unloaded quality factor $Q_u = 150$, we have the filter responses shown in Fig.8 as doted lines. The experimental results are also shown in Fig. 9 as solid lines that they are similar to the circuit model results except similar frequency drift as the former example. The frequency drift might come from the discrepancy of the substrate dielectric const. In other words, the dielectric const ε_r might be greater than data sheets' value 3.38.

From above two examples, we can conclude that the controlling line of source-load coupling can effectively adjusting the position of finite transmission zeros with negligible perturbation to the passband. It is suggested that one can design the symmetric folded coupled-resonator filter at first and then adds the controlling line to control the source-load coupling without fine-tuning other portion of the filter. The design method may apply to higher order symmetric folded coupled-resonator filter.

Ⅳ.Conclusion

. A novel diagnosis scheme has been proposed. Following a systematic design flow, two quadruplet filters with source-load

coupling where one was designed for quasi-elliptical and another was designed for flat group delay responses, were fabricated and the measured results agree well with that of theory. It has been shown that the diagnosis method described in this paper helps a lot to judge the unwanted effects in the microstrip quadruplet filter where these effects was usually very difficult to specify in microstrip's open environment.

Reference

1. R. J. Cameron, "Advanced coupling matrix synthesis techniques for microwave filters," *IEEE Trans. Microwave Theory Tech.*, vol. 51, pp.1-10, Jan. 2003.
2. H. -T Hsu, Z. Zhang, K. A. Zaki, and A. E. Atia, "Parameter extraction for symmetric coupled-resonator filters," in *Proc. IEEE MTT-S Int. Microwave Symp.*, vol. 3, June 2002, pp. 1445-1448
3. A. Garia-Lamperez, S. Llorente-Romano, M. Salazar-Palma, and T. K. Sarkar, " Efficient electromagnetic optimization of microwave filters and multiplexers using rational models,"IEEE Trans. Microwave Theory Tech., vol. 52, pp. 508-521, Feb. 2004.
4. A. E. Atia and H.-W. Yao, "Tuning and measurements of couplings and resonant frequencies for cascaded resonators," in *Proc. IEEE MTT-S Int. Microwave Symp.*, vol. 3, Boston, MA, June 2000, pp. 1637–1640.
5. A. Garia-Lamperez, S. Llorente-Romano, M. Salazar-Palma, M. Jesus Padilla-Cruz, and I. H. Carpintero, "Synthesis of cross-coupled lossy resonator filters with multiple input/output couplings by gradient optimization", *IEEE Antennas and Propagation Society International Symposium*, vol. 2, June 2003, pp. 52 - 55
6. H. C. Bell, Jr., "Canonical asymmetric coupled-resonator filters," *IEEE Trans. Microwave Theory Tech.*, vol. MTT-30, pp. 1333–1340, Sept.1982.
7. R. J. Cameron, "General coupling matrix synthesis methods for Chebychev filtering functions," *IEEE Trans. Microwave Theory Tech.*, vol. 47, pp. 433–442, Apr. 1999.
8. Giuseppe Macchiarella, "Accurate synthesis of inline prototype filters using cascaded triplet and quadruplet sections" *IEEE Trans. Microwave Theory Tech.*, vol. 50, pp. 1779–1783, July 2002.
9. Giuseppe Macchiarella, " A powerful tool for the synthesis of prototype filter with arbitrary topology" in *Proc. IEEE MTT-S Int. Microwave Symp.* , June 2003, pp. 1467-1470
10. J. S. Hong and M. J. Lancaster, *Microstrip Filters for RF/Microwave Applications.* New York: Wiley, 2001.
11. *Em User's Manual*, Sonnet Software Inc., Liverpool, NY, 2004.

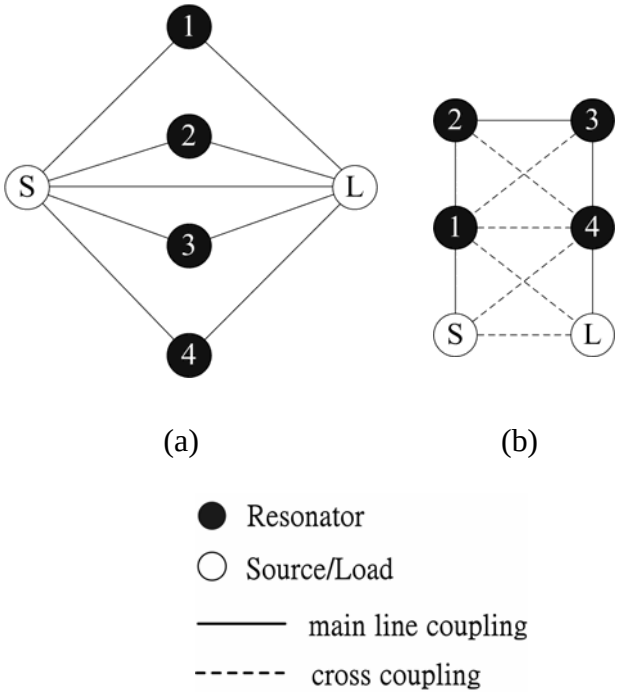

(a) (b)

Fig.1. Coupling routes of (a) a transversal filter, (b) a cross-coupled quadruplet filter with diagonal cross couplings.

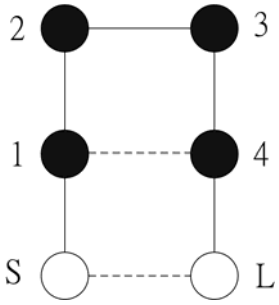

Fig.2 Coupling and routing scheme of symmetric cross-coupled quadruplet filter with source-load coupling

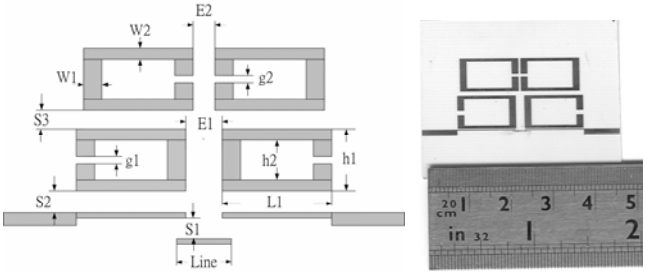

(a) (b)

Fig. 3(a) quadruplet filter with the capacitive S/L coupling controlled by the controlling line (b) photograph of the fabricated filter with dimension (in mils) S1=4, S2=8, S3=41, E1=90, E2=20, W1=64, W2=30, h1=310, h2=250, g1=42, g2=26, Line=160

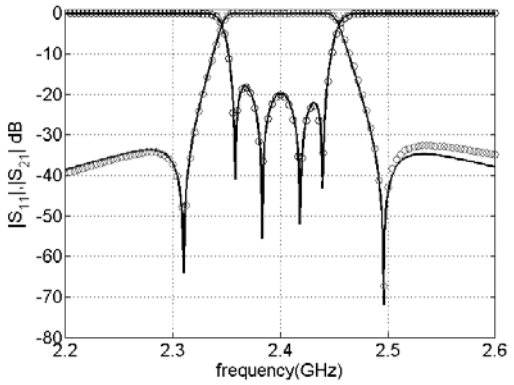

(a)

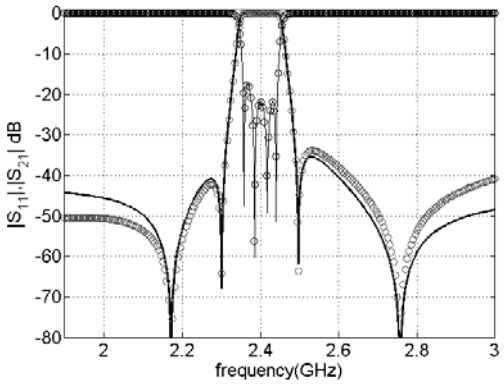

(b)

Fig.4 (a) response of quadruplet filter (b) response of quadruplet filter with controlling

line of source-load coupling. Circle: EM simulated results; solid line: circuit model.

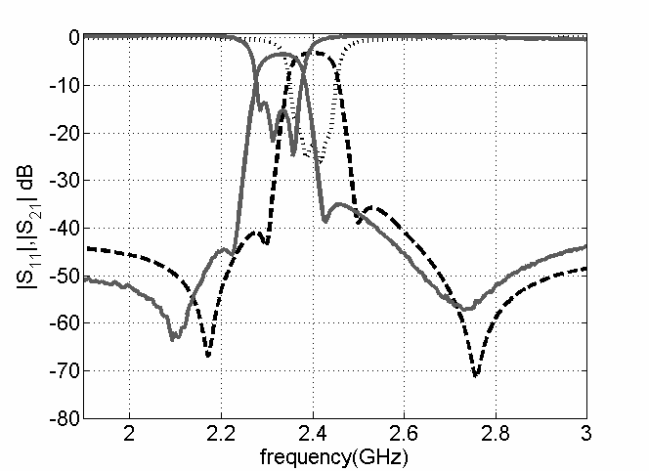

Fig.5 Experimental and circuit model results. Solid line: experimental results, dashed line: circuit model including loss term.

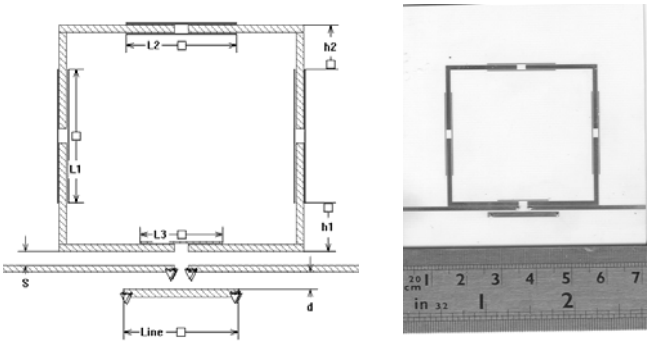

(a) (b)

Fig. 6 (a) quadruplet filter with the inductive S/L coupling controlled by the controlling line (b) photograph of the fabricated filter with dimension.d=20,Line=800,s=4,L3=575,L1=940,L2=770,L3=575,h1=340,h2=304 (in mil)

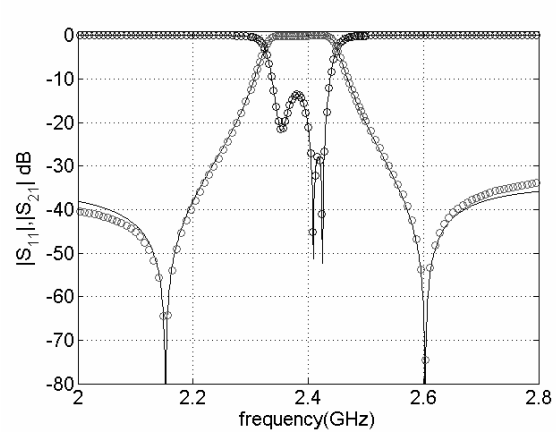

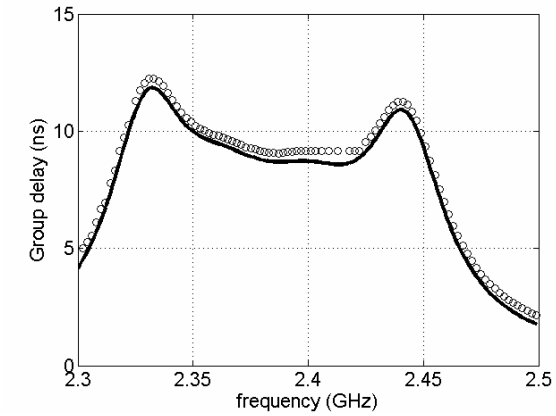

Fig. 7. Response of quadruplet filter with controlling line of source-load coupling. Circle: EM simulated results; solid line: circuit model.

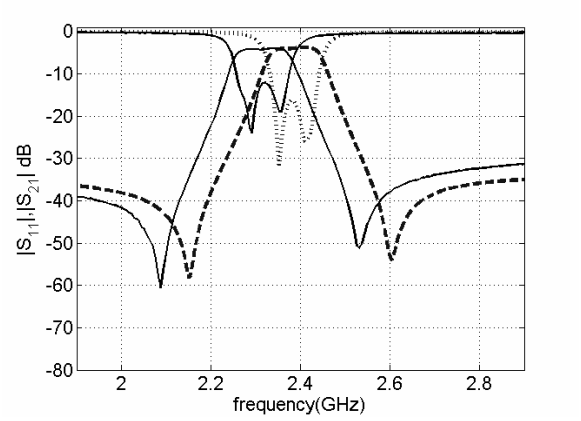

(a)

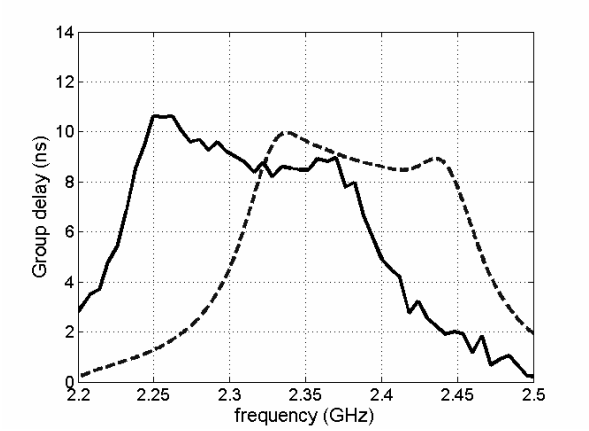

(b)

Fig.8 Experimental and circuit model results (a) return loss and insertion loss (b) group delay. Solid line: experimental results, dashed Line: circuit model including loss term.